Numerical Estimation of Frictional Effects in Equal Channel Angular Extrusion

Vinicius Aguiar de Souza, Ikumu Watanabe[*] and Akira Yanagida

National Institute for Materials Science (NIMS), Tsukuba 305–0047, Japan

The purpose of this study is to numerically estimate the friction coefficient for equal channel angular extrusion with and without back pressure. Three-dimensional finite element analysis is employed to estimate the coefficient of friction from the maximum pressing load, a crucial variable in die design. The finite element model consists of a billet, a plunger, a ram, and a die, where the interface between the billet and the die is modeled by the Coulomb friction model with truncated shear stress. The numerical model was validated by comparing the grid deformation patterns in the extrusion symmetry plane, and by comparing the load versus stroke curves for the ram (pressing load) and for the plunger (back pressure). Results indicate that the coefficient of friction can be accurately estimated from the maximum pressing load, but it is necessary to modify the traditional Coulomb friction model.   [doi:10.2320/matertrans.MH201513]

1. Introduction

Equal channel angular extrusion (ECAE), originally proposed by Segal *et al.*[1], is a popular forming process for fabricating bulk nanostructured materials (BNM). The extruded material presents enhanced mechanical properties such as high strength and superplasticity, which are caused by the severe plastic deformation (SPD) inflicted by the extrusion. In ECAE, a lubricated billet, with either a square or circular cross-section, can be repetitively extruded without changing the billet's geometry, through a die of equal channels that intersect each other at a fixed angle. The process is very popular in laboratories, but it does not have the same popularity in the industrial world. The reason is simple: ECAE can be scaled up for soft and easy-to-work materials, as demonstrated by Horita *et al.*[2], but is still far from being applied to a wider variety of commercial materials and to larger billets. The main impasse to extruding larger billets and difficult-to-work materials is how to properly design the die for industrial use.

As a result, many studies on ECAE have been published since Prangnell[3] published the first finite element analysis (FEA) of ECAE. The focus of the majority of the numerical investigations has been to understand the effect of parameters such as die geometry[4–8], billet geometry[9,10], ram speed[11,12], processing routes[13,14], temperature[9,15], and material properties[9,11,15,16] on the strain homogeneity of the extruded material. Many of these variables, including the die geometry, billet geometry, material properties, and processing route, are important for the die design. As yet, however, little attention has been paid to friction, a physical variable that is known to play a crucial role in extrusion even when the billet is lubricated, because it directly affects the deformation behavior, strain distribution, maximum pressing load and, consequently, the die design.

Attempts to characterize the effect of friction in strain homogeneity by employing three-dimensional finite element simulations of ECAE have been made by Suo *et al.*[17], Son *et al.*[18], Su *et al.*[19], Djavanroodi *et al.*[20], Nagasekhar *et al.*[21] and Si *et al.*[22] These studies present contradictory findings regarding how the friction affects the deformation behavior.

For instance, Suo *et al.*[17] provided evidence that the friction differently affects the strain homogeneity for each direction, and that the strain homogeneity increases with the friction. The fact that strain homogeneity increases with the increase in friction is corroborated by Su *et al.*[19] and Djavanroodi *et al.*[20] However, Si *et al.*[22] found that better strain homogeneity is achieved for low values of friction. Son *et al.*[18] found that the forming loads are dependent on the friction condition. Nagasekhar *et al.*[21] proved that it is possible to calculate the maximum peak load in ECAE by adjusting the coefficient of friction.

These studies have produced estimates of frictional effects on the deformation behavior of the billet as a function of a predefined range for the coefficient of friction. However, friction in ECAE is relatively constant; thus, a specific coefficient of friction value, which will be depend on the extruded material, must be obtained for proper die design. Furthermore, these studies opt for either of two distinct friction models: Coulomb or shear friction, without any justification for the choice of one in detriment of the other.

In this context, this study has two objectives. First, it aims to present an alternative model to numerically approach friction in ECAE while avoiding discrepancies between numerical and experimental data. Second, it aims to implement a method to estimate the coefficient of friction, which is essential for die design, for ECAE with and without back pressure. To accomplish these propositions, a three dimensional FEM model, symmetric in the lateral direction, is employed to estimate the coefficient of friction in ECAE with and without back pressure.

2. Finite Element Analysis

2.1 Finite element model and analysis conditions

The present study is focused on ECAE through a sharp die of a rectangular cross section with an angle of $90°$, under the effect of a hydrostatic back pressure (Fig. 1). All cases in this study employed a three-dimensional finite element model that was simulated using commercial Abaqus/Explicit code. A three-dimensional approach is elected because it provides a realistic approximation, i.e., it enables qualitative analysis of the material flow, deformation behavior, stress-strain distribu-
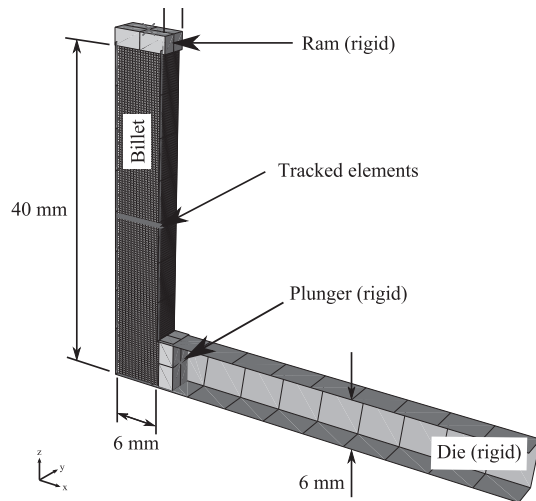
Fig. 1 Finite element model of ECAE and mirror symmetry on the *xz* plane are employed in this study. The elements tracked to acquire the strain distribution for the convergence analysis are highlighted.

Fig. 2 Stress-plastic strain curve of copper for simulation.

tion, load requirement, and frictional effects. A number of studies were systematically conducted *a priori* to define some of the simulation parameters, e.g., the number and type of elements, loading rates, and mass scaling, in terms of numerical error and computational time.

To decrease the computational cost, only the lateral half of the system (consisting of a billet, a die, a ram, and a plunger) was modeled while considering symmetrical boundary conditions (Y-plane). Because only the billet's deformation is considered, the die, the ram, and the plunger were modeled as rigid bodies employing rigid elements. The ram was constrained to move in the vertical direction (*z*-axis) with a velocity of 1 mm s^{-1}. The back pressure (176.06 MPa, the same value applied in the validation experiment) was applied uniformly on the head surface of the billet through the plunger, which was constrained to move in the horizontal direction (*x*-axis). The die consisted of inlet and outlet channels with an inner corner angle of $\phi = 90°$ and an outer corner angle of $\psi = 0°$. This study concentrated on this geometry because it provides the most homogeneous deformation and micro-structure development during ECAE[23,24].

The billet, with a square cross sectional area of 6×6 mm^2 and a length of 40 mm, was modeled using 55664 eight-node linear brick elements, based on a mesh convergence study. The billet was considered as commercially pure copper ($E = 130$ GPa, $\nu = 0.36$, $\rho = 8960$ kg m^{-3}) and modeled as an elastic-plastic material with von Mises yield criterion. The material properties were obtained from an uniaxial tension test (Fig. 2). The tension test was performed at the velocity of 0.5 mm min^{-1} using a rectangular tensile specimen made of pure copper (99.9 mass%) with dimensions 6.0 mm $\times$ 3.0 mm $\times$ 1.0 mm (gauge length, width, thickness), which was annealed for one hour at the temperature of 400°C. The Voce hardening law was employed to fit the experimental data and to extrapolate the strain values over 0.5, because they exceed this range during a single pass ECAE. The strain hardening behavior was assumed to be isotropic and independent of strain rate and temperature.

Because the billet's material properties are rate independent, increasing the loading rates (artificially elevating the
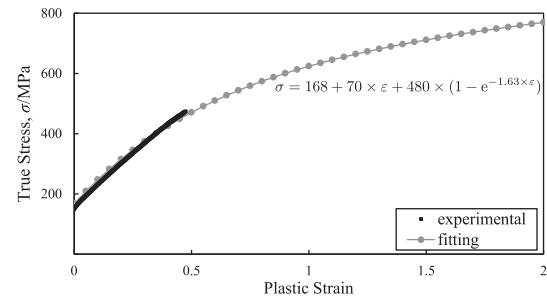
punch speed), and the mass scaling (artificially increasing the material density), can be employed to decrease the time required to simulate an explicit case. These two techniques can be employed as long as inertial effects caused by these increases are negligible. The significance of the inertial effects was analyzed by systematically comparing kinematic and internal energy, the overall deformation behavior, and the pressing load (load versus stroke curve) for a wide range of cases.

The penalty method and the Coulomb friction model with truncated shear stress[18,25] were employed to model the contact and friction on the interface between the billet and the die. In this study, the truncated shear stress is given as $\tau_{max} = \sigma_{y_o}/\sqrt{3}$ which does not depend on plastic hardening to simplify the friction modeling and its dependency on the load-stroke relationship, where σ_{y_o} is the Mises yield stress (for copper $\sigma_{y_o} = 168$ MPa obtained experimentally). To accommodate the large deformations, and consequently avoid the numerical instabilities generated by the severe mesh distortion, the model employed adaptive mesh refinement using the arbitrary Lagrangian-Eulerian (ALE) method. Additionally, heat supposedly generated from the contact (friction) and the deformation were neglected.

2.2 Validation of the FE model

An ECAE experiment was conducted on commercially pure copper to validate the FEM analysis. The samples were prepared with the same cross sectional area as the numerical model and extruded in a steel die with the same geometry as its numerical counterpart, i.e., $\phi = 90°$, $\psi = 0°$. In order to decrease frictional effects, Teflon based lubricant was applied in both the die and billet before the extrusion, after which the samples were extruded at room temperature by a ram with a constant speed of 1 mm s^{-1}. During the extrusion, with a total stroke of 30 mm, a hydrostatic force of 6.34 kN (back pressure = 176.06 MPa) was applied to the billet's head using an hydraulic actuator. Both the pressing load required to extrude the billet and the hydrostatic back pressure were recorded for verification of the numerical model. Moreover, a grid was engraved by employing electrolytic marking in the *y* plane, to evaluate the grid deformation behavior as an extra variable for model verification as suggested by Bowen *et al.*[4] The validation of the numerical model was conducted by comparing two aspects of the experimental and numerical results; these included:

i a comparison of the grid deformation patterns in the symmetry plane of the extruded sample and the corresponding finite element analysis (Fig. 3), and

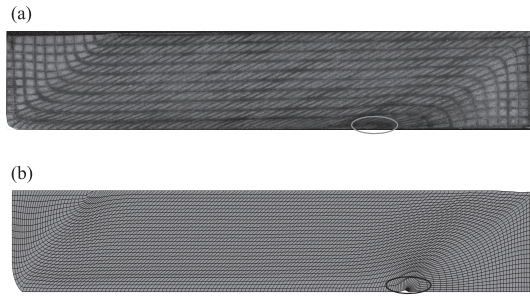ii a comparison of the load versus stroke curves for the ram

(a)

(b)

Fig. 3 Comparison of grid deformation in the experiment and numerical simulation. (a) Experimental results, (b) Numerical results.
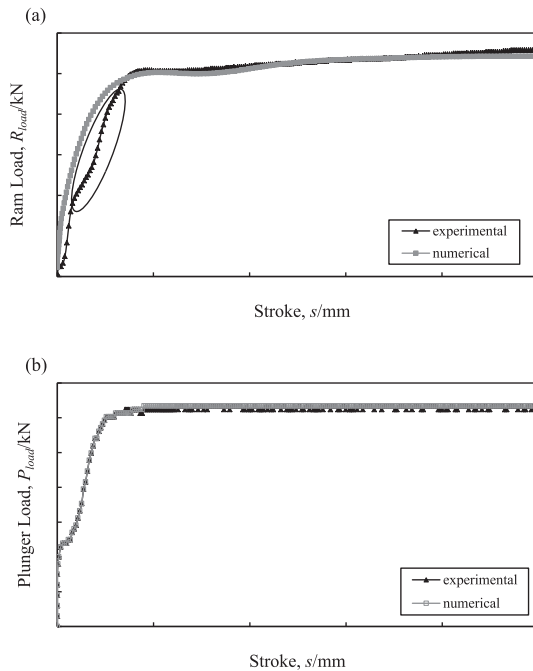
(a)

Stroke, s/mm

(b)

Stroke, s/mm

Fig. 4 Recorded ram and plunger loads and a comparison of load versus stroke curves between experimental and numerical simulation (study case: commercially pure copper billet extruded at 1 mm s^{-1}, $\phi = 90°$, $\psi = 0°$, $\mu = 0.021$). The circled region is caused by the small difference between the inlet channel width and the billet's dimensions. (a) Comparison for the ram, (b) Comparison for the plunger.

(pressing load) and the plunger (back pressure) obtained experimentally and numerically (Fig. 4).

The first aspect was analyzed by simply comparing Figs. 3(a) and 3(b). The finite element results emulated the overall behavior of the extruded sample, presenting a reasonable level of agreement between grid deformation patterns for all three main areas of the sample: the head, the steady state zone, and the tail. Clearly, aside from a small deformation caused by the compression/upsetting, the tail experienced no significant deformation. This is expected because the region does not pass through the plastic deformation zone in the intersection of the outer and inner corners. Following the example of the tail, the head was hardly deformed by shear because it had already effectively passed through the plastic deformation zone, and the small deformation observed in this region was caused entirely by the back pressure. On the other hand, the steady state region presented a very uniform strain distribution inflicted by the dominant deformation mode; i.e., the single shear produced in the junction between the outer and inner corners deformed this region under almost steady state conditions. Additionally, both results presented a formation of a fragment in the bottom part of the billet. This fragment was a result of a severe deformation that appears at the bottom (the region is circled in Figs. 3(a) and 3(b)), which was formed at the early stage of the ECAE process as the material in the region folded over itself.

The second aspect was analyzed by comparing the load versus stroke curves in the experimental and FEM predicted results for the ram (pressing load) and the plunger (back pressure). It is possible to observe that they present an excellent level of agreement, with similar trends, as can be seen in Figs. 4(a) and 4(b). The trend shows that the curve has a very steep slope until the yield limit is reached, after which this slope decreases drastically as the material flows through the second channel. Nevertheless, a small discrepancy was observed in the ram case results that is not significant enough to introduce a substantial error. This difference is mainly due to the small gap that exists between the sample and the inlet channel, which is caused by the difference between the inlet channel width and the billet's dimensions. This gap is primarily filled by the billet's upsetting, and generates the small change in slope in the curve (the region is indicated in Fig. 4(a)).

3. Results and Discussion

The results of the present work are discussed in terms of a method to estimate the coefficient of friction based on the maximum pressing load, which is obtained from the load versus stroke curves for cases with and without back pressure. A precise estimation of the coefficient of friction is important, because the friction plays an important role in the deformation behavior, strain distribution and maximum pressing load that occur during ECAE.

3.1 Determination of the coefficient of friction in ECAE

Prior studies have reported the relationship between the maximum pressing load and the coefficient of friction. Xu *et al.*[26] found a linear relation for these variables while Esmailzadeh *et al.*[27] presented a third degree polynomial to relate them. However, these two studies do not go further in estimating the coefficient of friction for ECAE. A remarkable initiative to calculate the coefficient of friction for this process was proposed by Nagasekhar *et al.*[21] and Patil *et al.*[28] The first step in their approach is to obtain by FEM a series of curves representing the pressing load versus the stroke for a predefined range of the coefficients of friction. All obtained curves are plotted in the same graph, as depicted in Fig. 5(a). In this study, the coefficient of friction ranges from $\mu = 0$ to $\mu = 0.075$ in increments of 0.025. This initial estimate is based on typical coefficient of friction values for cold metal forming, as stressed in the work of Kim[29].

The second step is to find the points of local maximum in each of the curves in Fig. 5(a); this is calculated using the condition $\frac{d}{ds}R_{load} = 0$ and $\frac{d^2}{ds^2}R_{load} < 0$, where R_{load} is the ram pressing load and s is the stroke. From these maxima, a curve representing the maximum pressing load versus the coefficient of friction is obtained, as depicted in Fig. 5(c). This is an excellent idea; however, the numerical pressing load predict-
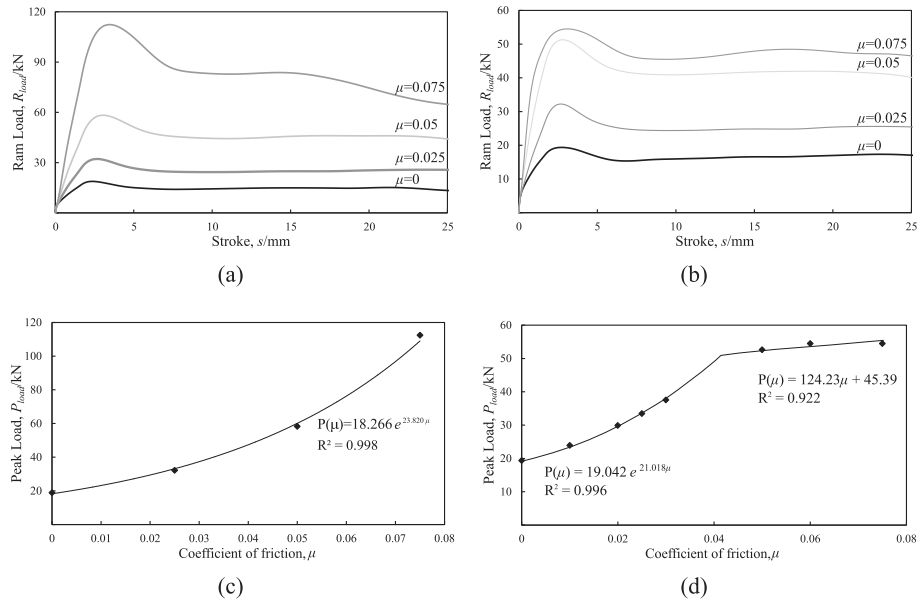
Fig. 5 A comparison of (a) Coulomb and (b) maximum shear approaches for the load required to extrude the billet through the channels for four friction conditions, and a comparison of the Coulomb (c) and maximum shear (d) approaches for the maximum pressing load versus coefficient of friction, μ.
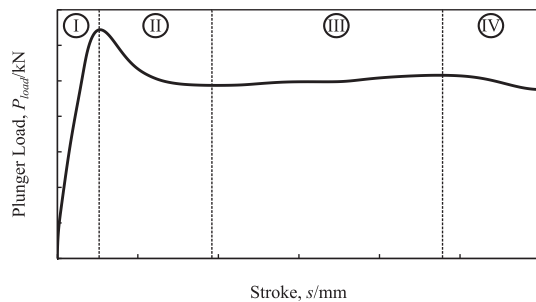

Fig. 6 Typical pressing load stages on ECAE obtained in numerical simulation (study case: commercially pure copper billet extruded at 1 mm s^{-1}, $\phi = 90°$, $\psi = 0°$, $\mu = 0.025$).

ed in their independent studies presented some discrepancies for the third and fourth stages of ECAE (Fig. 6). For these two stages, the numerical pressing load decreases continuously; this is not observed in their ECAE experimental results or in results of similar experiments conducted by Son *et al.*[18], and Aour *et al.*[30]

The disparities observed can be attributed to the Coulomb friction model employed in their numerical study. This approach assumes that the frictional effects are a specific function of the normal contact stresses, which keep these forces constant for the entire process. In the cases depicted in Fig. 5(a), an increase in the coefficient of friction yields an increase in the pressing load. Considering only the maximum pressing load on these curves, the results indicate that the coefficient of friction has an exponential dependency on the maximum pressing load, i.e., $P(\mu) = 18.266e^{23.820\mu}$, which seems physically improbable. This is a clear indication that the Coulomb friction model is not appropriate for simulating this process, a fact also stressed by Balasundar and Raghu[25].

A better approach to model the friction would be defining a maximum shear stress, as suggested in this work. In this approach, if the friction shear stress exceeds the maximum value defined, the friction stress is always maintained at a level lower than the yield stress of the material in pure shear.

Although the two friction models predicted similar results for the low friction cases, the results for the cases with relatively high friction ($\mu > 0.05$) are quite different. Comparing Fig. 5(a) to Fig. 5(b), it is clear to notice that the second approach maintains the pressing load within a certain limit, because the relations between the pressing load, the maximum pressing load, and the coefficient of friction present an asymptotic behavior (Fig. 5(d)). It is important to mention that the coefficient of friction can still be calculated from the fitting obtained from the correlation depicted in Fig. 5(d).

3.2 Determination of the coefficient of friction in ECAE with back pressure

The same method and friction model can also be applied to cases of ECAE with back pressure (Fig. 7). The pressing loads obtained for these cases are different from those in the previous cases, in which four stages can be distinguished. The only similarity between the cases with and without back pressure is that they all maintain the curve's original shape ($\mu = 0$), which is amplified according to the frictional effect until the asymptotic limit. In the previous cases, the maximum pressing load, i.e., the absolute maximum, served to estimate the coefficient of friction; however in the back pressure case this value is not clearly identifiable. In order to choose appropriately, it is necessary to define where this point must be selected.

An acceptable solution is to use the local maximum that corresponds to the beginning of the steady state for the plastic strain distribution by employing $\frac{d}{ds}L_{steady\ state} = 0$ and $\frac{d^2}{ds^2}L_{steady\ state} < 0$, as in the previous case. The steady state deformation is achieved numerically around a total stroke of 5 mm, so that the corresponding maximum pressing load can be identified for each case in Fig. 7(a). The next step is to plot a graph of this local maximum pressing load versus the coefficient of friction, and fit an appropriate function to the data.

Thus, using the experimental data acquired in this study and the correlation calculated from the FE model (Fig. 7(b)), it is possible to estimate the coefficient of friction during
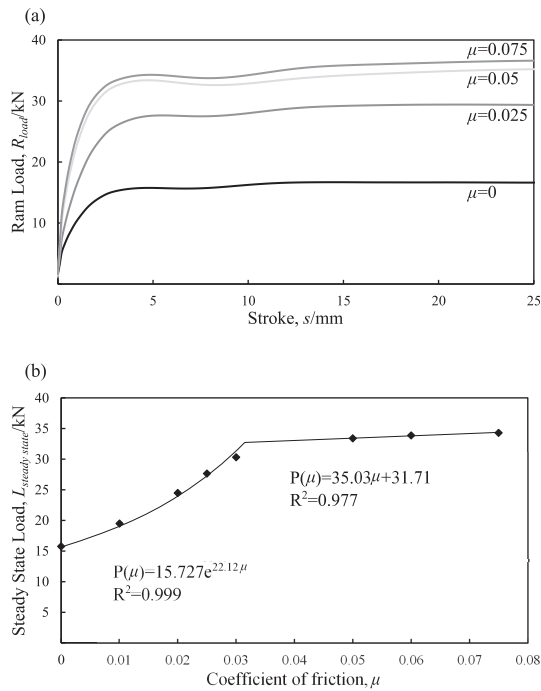
(a)

(b)

Fig. 7 (a) the load required to extrude the billet through the channels for four friction conditions, and (b) the steady state load versus coefficient of friction for a case with a back pressure of 176.056 MPa.

ECAE for copper as $\mu = 0.021$. This value has a percentage error of 5% in relation to the experimental value of 0.02 estimated by Smolyakov *et al.*[31] The method of this study was also applied to pure aluminum. Contrary to the case already discussed, the graphics for the pure aluminum case are not presented, to maintain the conciseness of this work. For this case, the estimated coefficient of friction during ECAE is $\mu = 0.125$, with a percentage error of 4.2% in relation to the value $\mu = 0.12$ suggested by Djavanroodi and Ebrahimi[20] and Jung *et al.*[32]

4. Conclusion

This study has systematically proven that the friction model affects the pressing load (load versus stroke curve), which is an important variable for ECAE system (tool and die) design. Consequently, the friction model must be carefully selected in 3D FE simulations. Additionally, this study confirmed that the pressing load (load versus stroke curve) should be employed to estimate the coefficient of friction during a single pass ECAE of pure copper and pure aluminum. However, it is necessary to modify the traditional Coulomb friction model, which is popularly employed in ECAE simulations, to include the material maximum shear stress value. This yields better agreement with the experiments and a more realistic representation of the frictional effects. Additionally, the method is extended to ECAE with a back pressure for which a distinct value, based on steady state zone formation, must be chosen to find the correlation with the coefficient of friction. The accuracy of the improved and extended method is supported by the small margin of error between experimental and numerical results. A limitation of this study is that the the FE model was validated by performing a qualitative analysis of the grid deformation patterns between experimental and numerical results. Although the results present a reasonable agreement, a better option would be to perform a digital image correlation analysis (DIC).

REFERENCES

1) V.M. Segal, V.I. Reznikov, A.E. Drobyshevskii and V.I. Kopylov: Russ. Metall. **1** (1981) 99–105.
2) Z. Horita, T. Fujinami and T.G. Langdon: Mater. Sci. Eng. A **318** (2001) 34–41.
3) P.B. Prangnell, C. Harris and S.M. Roberts: Scr. Mater. **37** (1997) 983–989.
4) J.R. Bowen, A. Gholinia, S.M. Roberts and P.B. Prangnell: Mater. Sci. Eng. A **287** (2000) 87–99.
5) H.S. Kim, M.H. Seo and S.I. Hong: J. Mater. Process. Technol. **130** (2002) 497–503.
6) A.V. Nagasekhar and Y. Tick-Hon: Comput. Mater. Sci. **30** (2004) 489–495.
7) J.-H. Lee, I.-H. Son and Y.-T. Im: Mater. Trans. **45** (2004) 2165–2171.
8) W. Wei, A.V. Nagasekhar, G. Chen, Y. Tick-Hon and K.X. Wei: Scr. Mater. **54** (2006) 1865–1869.
9) H.S. Kim, P. Quang, M.H. Seo, S.I. Hong, K.H. Baik, H.R. Lee and D.M. Nghiep: Mater. Trans. **45** (2004) 2172–2176.
10) S.C. Yoon, M.H. Seo and H.S. Kim: Scr. Mater. **55** (2006) 159–162.
11) H.S. Kim, M.H. Seo and S.I. Hong: Mater. Sci. Eng. A **291** (2000) 86–90.
12) S.W. Chung, W.-J. Kim, M. Kohzu and K. Higashi: Mater. Trans. **44** (2003) 973–980.
13) T. Suo, Y. Li, Q. Deng and Y. Liug: Mater. Sci. Eng. A **466** (2007) 166–171.
14) C.W. Su, L. Lu and M.O. Lai: Mater. Sci. Technol. **23** (2007) 727–735.
15) D.P. Delo and S.L. Semiatin: Metallurgical and Materials Transactions A 30 (1999) 1391–1402.
16) S.L. Semiatin, D.P. Delo and E.B. Shell: Acta Mater. **48** (2000) 1841–1851.
17) T. Suo, Y. Li, Y. Guo and Y. Liu: Mater. Sci. Eng. A **432** (2006) 269–274.
18) I.H. Son, Y.G. Jin, Y.T. Im, S.H. Chon and J.K. Park: Mater. Sci. Eng. A **445** (2007) 676–685.
19) C.W. Su, L. Lu and M.O. Lai: Mater. Sci. Technol. **23** (2007) 727–735.
20) F. Djavanroodi and M. Ebrahimi: Mater. Sci. Eng. A **527** (2010) 1230–1235.
21) A.V. Nagasekhar, S.C. Yoon, Y. Tick-Hon and H.S. Kim: Comput. Mater. Sci. **46** (2009) 347–351.
22) J.Y. Si, F. Gao and J. Zhang: Journal of Iron and Steel Research **19** (2012) 54–58.
23) S. Li, M.A.M. Bourke, I.J. Beyerlein, D.J. Alexander and B. Clausen: Mater. Sci. Eng. A **382** (2004) 217–236.
24) S.J. Oh and S.B. Kang: Mater. Sci. Eng. A **343** (2003) 107–115.
25) I. Balasundar and T. Raghu: Mater. Des. **31** (2010) 449–457.
26) S. Xu, G. Zhao, X. Ma and G. Ren: J. Mater. Process. Technol. **184** (2007) 209–216.
27) M. Esmailzadeh and M. Aghaie-Khafri: Comput. Mater. Sci. **63** (2012) 127–133.
28) B.V. Patil, U. Chakkingal and T.S.P. KumarPrasanna: 17th International Conference on Metallurgy and Materials 2008 (2008) 1–9.
29) H.S. Kim: Mater. Sci. Eng. A **430** (2006) 346–349.
30) B. Aour, F. Zaïri, R. Boulahia, M. Naït-Abdelaziz, J.-M. Gloaguen and J.-M. Lefebvre: Comput. Mater. Sci. **45** (2009) 646–652.
31) A.A. Smolyakov, V.P. Solovyev, A.I. Korshunov and N.A. Enikeev: Mater. Sci. Eng. A **493** (2008) 148–159.
32) K.-H. Jung, D.-K. Kim, Y.-T. Im and Y.-S. Lee: Int. J. Plast. **42** (2012) 120–140.